Are historical records sufficient to constrain ENSO simulations?

Andrew T. Wittenberg[1]

[1] A control simulation of the GFDL CM2.1 global coupled GCM, run for 2000 years with its atmospheric composition, solar irradiance, and land cover held fixed at 1860 values, exhibits strong interdecadal and intercentennial modulation of its ENSO behavior. To the extent that such modulation is realistic, it could attach large uncertainties to ENSO metrics diagnosed from centennial and shorter records – with important implications for historical and paleo records, climate projections, and model assessment and intercomparison. Analysis of the wait times between ENSO warm events suggests that such slow modulation need not require multidecadal memory; it can arise simply from Poisson statistics applied to ENSO's interannual time scale and seasonal phase-locking. **Citation:** Wittenberg, A. T. (2009), Are historical records sufficient to constrain ENSO simulations?, *Geophys. Res. Lett.*, *36*, L12702, doi:10.1029/2009GL038710.

1. Introduction

[2] The El Niño/Southern Oscillation (ENSO) is Earth's dominant interannual climate fluctuation, affecting agriculture, ecosystems, and weather around the globe. Yet the future of ENSO remains uncertain, with a large spread of model projections for the 21st century [*Guilyardi et al.*, 2009]. Historical SST reconstructions (e.g., Figure 1a) indicate multidecadal variations in ENSO behavior, but these extend only back to the mid-19th century and must cope with sparse and changing observing systems. Paleo-proxy records also suggest past modulation of ENSO [*Cane*, 2005], but sampling of corals, lake sediments, and tree rings remains limited, and they can in some cases confound ENSO changes with changes in local climate or in ENSO's teleconnections to the proxy sites.

[3] Simplified ENSO models have long been capable of producing irregular ENSOs [*Cane et al.*, 1995; *Wittenberg*, 2002; *Timmermann et al.*, 2003; *An et al.*, 2008; *Kleeman*, 2008; *Fang et al.*, 2008], as have coarse-resolution and flux-adjusted coupled GCMs (CGCMs) [*Knutson et al.*, 1997; *Timmermann et al.*, 1999; *Yukimoto and Kitamura*, 2003; *Min et al.*, 2005; *Brown et al.*, 2008]. However, only recently has available computer power permitted CGCMs with fairly realistic ENSOs to run for millennia, without flux adjustments and with little climate drift.

[4] The dearth of long ENSO records from observations and CGCMs leaves key questions unanswered. In the absence of external perturbations, what is the likelihood of extended epochs of unusual ENSO variations? What causes these epochs, and are they predictable? How long a record is needed to distinguish an ENSO simulation from observations or another simulation, or to discern impacts of a change in physical parameters or climate forcings?

[5] Here we present a CGCM simulation that exhibits long modulation time scales for ENSO. While our immediate goal is to describe this model's sampling variability – for later use in detecting impacts of climate forcings and model development – our broader objective is to spur the climate community to consider long-term modulation of ENSO in other models, observations, and paleoclimate records.

2. Experiment

[6] The Geophysical Fluid Dynamics Laboratory (GFDL) CM2.1 global coupled atmosphere/ocean/land/ice GCM is described by *Delworth et al.* [2006, and references therein]. CM2.1 played a prominent role in the third Coupled Model Intercomparison Project (CMIP3) and the Fourth Assessment of the Intergovernmental Panel on Climate Change (IPCC), and its tropical and ENSO simulations have consistently ranked among the world's top GCMs [*van Oldenborgh et al.*, 2005; *Wittenberg et al.*, 2006; *Guilyardi*, 2006; *Reichler and Kim*, 2008]. The coupled pre-industrial control run is initialized as by *Delworth et al.* [2006], and then integrated for 2220 yr with fixed 1860 estimates of solar irradiance, land cover, and atmospheric composition; we focus here on just the last 2000 yr. This simulation required one full year to run on 60 processors at GFDL.

3. Results

3.1. NINO3 SST Time Series

[7] Figure 1b shows the resulting 20 centuries of simulated pre-industrial SSTs, averaged over the NINO3 region (150°W–90°W, 5°S–5°N) in the heart of the interannual SST variability in both CM2.1 and the observations. CM2.1, which runs without flux adjustments, produces very little drift in its simulated NINO3 time-mean SST: the second millennium is only 0.1°C warmer than the first. The simulated 2000 yr mean is slightly cooler than observed over 1876–1975, due to both the absence of increasing greenhouse gases and a CM2.1 cold bias evident even in 20th-century simulations [*Wittenberg et al.*, 2006].

[8] The modulation of the CM2.1 ENSO is striking. There are multidecadal epochs with hardly any variability (M5); epochs with intense, warm-skewed ENSO events spaced five or more years apart (M7); epochs with moderate, nearly sinusoidal ENSO events spaced three years apart (M2); and epochs that are highly irregular in amplitude and period (M6). Occasional epochs even mimic detailed temporal sequences of observed ENSO events; e.g., in both R2

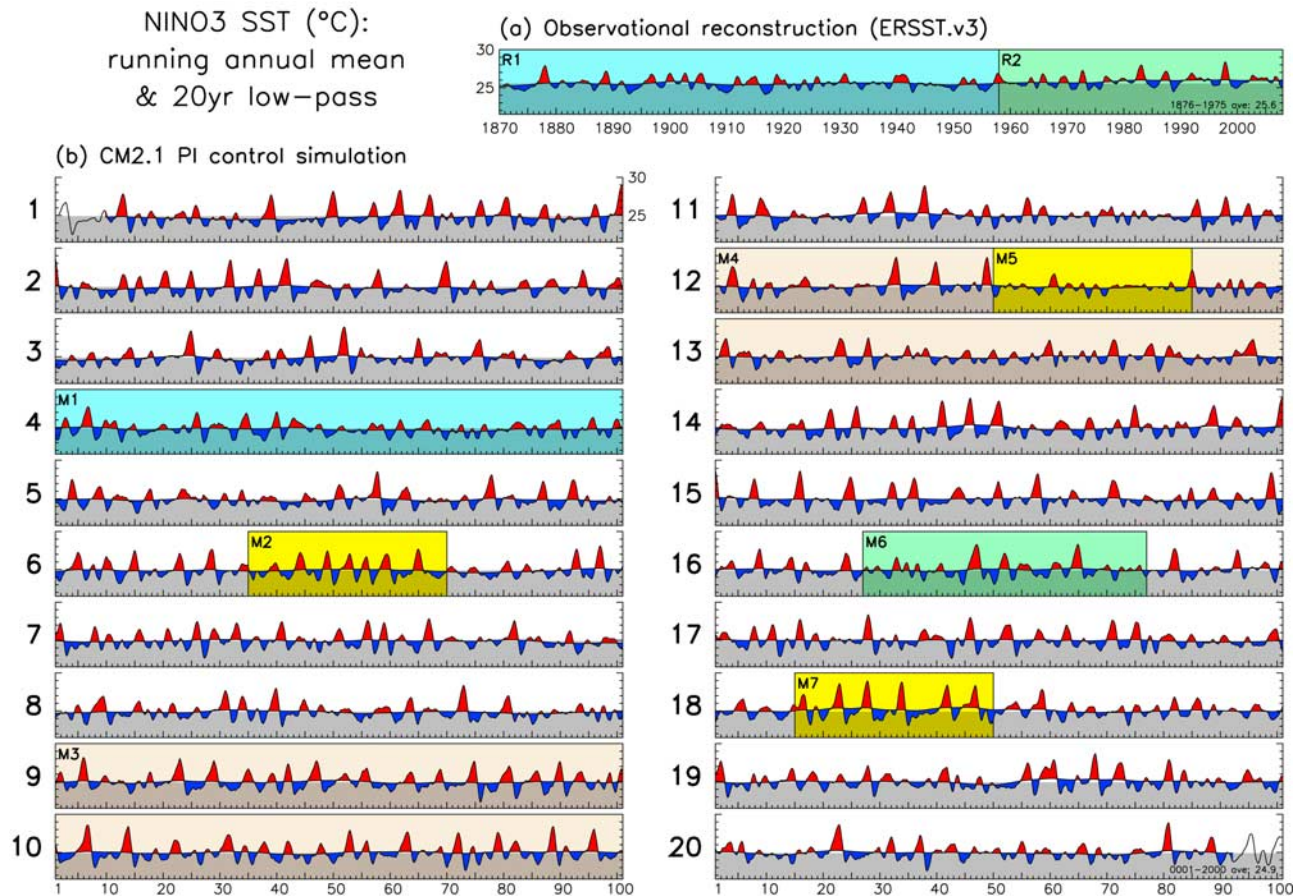[1]Geophysical Fluid Dynamics Laboratory, NOAA, Princeton, New Jersey, USA.

Figure 1. SST (°C) averaged over the NINO3 region (150°W–90°W, 5°S–5°N), for (a) the ERSST.v3 historical reconstruction of *Smith et al.* [2008], and (b) the 20 consecutive centuries (numbered) from the CM2.1 pre-industrial control run. Red/blue shading highlights departures of the running annual-mean SST from the multidecadal background state, where the latter is obtained via a 211-month triangle smoother which transmits (25, 50, 75)% of the time series amplitude at periods of (15, 20, 30) yr. Unshaded time series ends in Figure 1b indicate the half-width of the triangle smoother; ends of the observed time series in Figure 1a are zero-padded prior to smoothing. The top of the gray bar is the long-term mean, indicated at the bottom right of each plot. Labeled epochs are discussed in the text.

and M6, there are decades of weak, biennial oscillations, followed by a large warm event, then several smaller events, another large warm event, and then a long quiet period. Although the model's NINO3 SST variations are generally stronger than observed, there are long epochs (like M1) where the ENSO amplitude agrees well with observations (R1). An unlucky modeler – who by chance had witnessed only M1-like variability throughout the first century of simulation – might have erroneously inferred that the model's ENSO amplitude matched observations, when a longer simulation would have revealed a much stronger ENSO.

[9] If the real-world ENSO is similarly modulated, then there is a more disturbing possibility. Had the research community been unlucky enough to observe an unrepresentative ENSO over the past 150 yr of measurements, then it might collectively have misjudged ENSO's longer-term natural behavior. In that case, historically-observed statistics could be a poor guide for modelers, and observed trends in ENSO statistics might simply reflect natural variations.

[10] The modulation time scales of the CM2.1 ENSO are surprisingly long. A 200 yr epoch of consistently strong

variability (M3) can be followed, just one century later, by a 200 yr epoch of weak variability (M4). Documenting such extremes might thus require a 500+ yr record. Yet few modeling centers currently attempt simulations of that length when evaluating CGCMs under development – due to competing demands for high resolution, process completeness, and quick turnaround to permit exploration of model sensitivities. Model developers thus might not even realize that a simulation manifested long-term ENSO modulation, until long after freezing the model development. Clearly this could hinder progress. An unlucky modeler – unaware of centennial ENSO modulation and misled by comparisons between short, unrepresentative model runs – might erroneously accept a degraded model or reject an improved model.

3.2. Modulation of NINO3 Spectra

[11] Figure 2a shows time-mean spectra of the observations in Figure 1a, for epochs of length 20 yr – roughly the duration of observations from satellites and the Tropical Atmosphere Ocean (TAO) buoy array. The spectral power is fairly evenly divided between the seasonal cycle and the
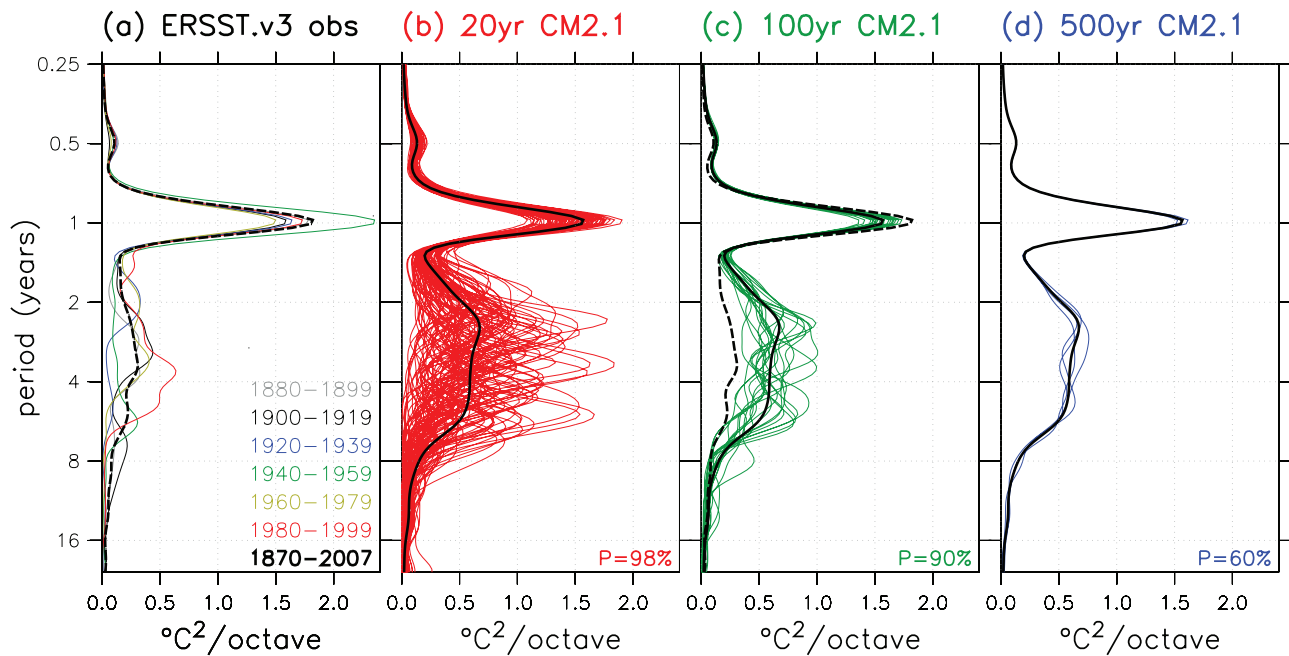
Figure 2. Power spectra of NINO3 SSTs, as a function of the period in octaves of the annual cycle. These spectra are computed by time-averaging the spectral power density from a Morlet wavenumber-6 wavelet analysis, and preserve energy in that the area to the left of each curve represents the spectral power within a frequency band. (a) Spectra for six 20 yr epochs (solid) and one 138 yr epoch (dashed and repeated in Figure 2c) from the ERSST.v3 observational reconstruction. Spectra from the CM2.1 control simulation; thick black solid line is the average spectrum for the full 2000 yr run, and thin colored lines are the N subspectra from non-overlapping epochs of length (b) 20 yr ($N = 100$), (c) 100 yr ($N = 20$), and (d) 500 yr ($N = 4$). Were the simulated subspectra independent and identically distributed, the extrema of the N subspectra at each time scale would comprise a prediction interval for the next subspectrum; at bottom right is the probability $P = (N - 1)/(N + 1)$ that an interval so constructed would bracket the next subspectrum to emerge from the model.

interannual ENSO band, the latter spanning a broad range of time scales between 1.3 to 8 yr. Amplitude modulation is present throughout the spectrum, most prominently in the ENSO band where 20 yr spectra exhibit large fractional deviations from the 138 yr mean. Figure 2b shows corresponding spectra for 20 yr records from the CM2.1 control run. While the CM2.1 ENSO spectrum is clearly stronger than observed, its fractional amplitude modulation is fairly realistic. For 20 yr epochs, annual cycle variance between 0.9–1.1 yr is anticorrelated with ENSO variance between 1.5–6 yr (−0.48 correlation in CM2.1, −0.66 in observations).

[12] For century-long records – approaching the limits of historical SST reconstructions like Figure 1a – the inter-epoch spread of spectra shrinks by a factor of roughly $(100/20)^{1/2} = 2.2$ compared to the 20 yr spectra, as expected for independent estimates of the spectrum. The observed 138 yr record can now clearly be distinguished from the model at annual and interannual time scales. Yet there remains a large spread among centennial spectra, with the extremes (which comprise a 90% prediction interval for the next centennial spectrum) still spanning a factor of 2 in power in the interannual band. Only for records of 500 yr or more does the sampling variability fall to a small fraction of the total interannual power.

3.3. A Null Hypothesis for ENSO Modulation

[13] What causes the long-term modulation of ENSO in the CM2.1 control run? One possibility is that ENSO

stability is altered by decadal and longer-scale changes in climate, arising either from ENSO itself, or from outside the tropical Pacific (e.g., the Atlantic or North Pacific). Yet the CM2.1 tropical climate shows hardly any centennial-mean change in SST between the active (M3) and inactive (M4) epochs of Figure 1; the largest change is in the western equatorial Pacific, where the active M3 epoch is cooler than M4 by just 0.3°C in SST and 0.1°C over the top 300 m (not shown). Small background changes could conceivably drive large centennial variations in the CM2.1 ENSO, were the system positioned near a bifurcation point (currently unknown). However, the background changes could themselves arise from ENSO modulation: in CM2.1 as in nature, SST anomalies during El Niño are stronger and peak farther east than during La Niña – giving a residual time-mean SST that is warm in the east Pacific and cold in the west during active-ENSO epochs (e.g., M7 in Figure 1b). *Jin et al.* [2003], *Rodgers et al.* [2004], and *Schopf and Burgman* [2006] have all pointed to such nonlinear rectification of ENSO as a prominent source of decadal-scale Pacific SST variations.

[14] An alternative hypothesis for the long-term ENSO modulation in CM2.1 is that it arises stochastically, from nothing more than ENSO's interannual time scale and seasonal phase-locking. Consider an idealized stochastic process in which events occur independently (memory-lessly) of one another in time, with a fixed probability of an event occurring at any instant, and a mean inter-event
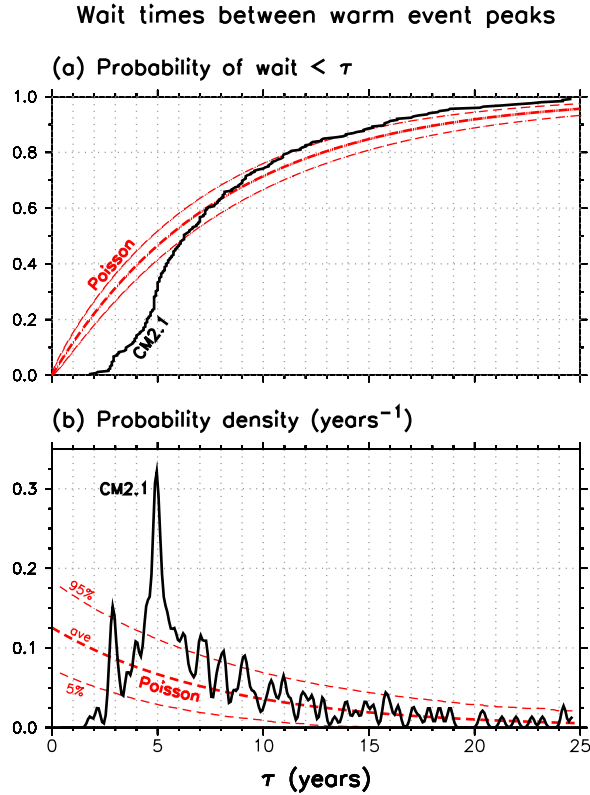
Wait times between warm event peaks

(a) Probability of wait < τ

(b) Probability density (years⁻¹)

Figure 3. Distribution of wait times between moderate-to-strong warm event peaks, for CM2.1 (black line) and a Poisson process with CM2.1's average wait time of 8 yr (red lines). (a) Probability that wait time does not exceed time τ; (b) probability density of wait times, smoothed using a Gaussian kernel with a 2-month e-folding halfwidth. Poisson percentiles are computed from 100,000 Monte Carlo realizations of 250 Poisson events, processed just like the 250 CM2.1 events.

time $\overline{\tau}$. The inter-event wait times τ for this homogeneous Poisson process are exponentially distributed:

$$p(\tau) = \frac{1}{\overline{\tau}} e^{-\tau/\overline{\tau}} \quad (1)$$

whose integral is the cumulative distribution

$$P(wait < \tau) = 1 - e^{-\tau/\overline{\tau}} \quad (2)$$

We expect occasional long inactive epochs from such a process, since (for example) the probability of waiting longer than $3\overline{\tau}$ between events is $1 - P(wait < 3\overline{\tau}) = e^{-3} = 5\%$.

[15] To identify CM2.1 events, we remove a monthly climatology from the 2000 yr time series of NINO3 SSTs, and then smooth the resulting anomalies with an 11-month triangle smoother that transmits (25, 50, 75)% of the time series amplitude at periods of (0.8, 1.1, 1.7) yr. We then search the anomaly time series for moderate-to-strong warm events exceeding one standard deviation (1.1°C) for at least 4 months. For each of the 250 such events, we record the month of peak warm anomaly, and the time to the next warm event peak.

[16] The CM2.1 wait-time distribution (Figure 3) is highly skewed, with a most common wait of 5 yr, a mean of $\overline{\tau} = 2000yr/250 = 8$ yr, and a (20, 50, 80)% chance of waiting less than (4.5, 6.3, 11.2) yr. In contrast to the Poisson events, the CM2.1 events occur at least 1.3 yr apart – due to the slow recharge, following a warm event, of west Pacific warm pool heat content via off-equatorial Sverdrup adjustment and gradual surface-flux heating [*Jin*, 1996; *Yukimoto and Kitamura*, 2003]. CM2.1 also favors an integral number of years between events – due to the seasonal phase-locking of ENSO, and reminiscent of quasi-periodicity seen in simple and intermediate-complexity ENSO models [*Jin et al.*, 1994; *Tziperman et al.*, 1995].

[17] The CM2.1 annual peaks at 3, 5, 7, 8, and 9 yr all exceed the Poisson 95% limits, suggesting that NINO3 SST may retain some memory of past warm events for up to a decade. But beyond 10 yr, the CM2.1 wait times are indistinguishable from those of a Poisson process, with no evidence of inter-event memory in CM2.1 NINO3 SSTs at multidecadal time scales. Yet 15% of the Poisson events, and 10% of the CM2.1 warm events, occur more than 15 yr after their predecessors, and waits of 24 yr ($3\overline{\tau}$) can be found in CM2.1. Thus even a memoryless interannual process can occasionally produce very long wait times between El Niños, resulting in apparent ENSO modulation.

4. Summary and Discussion

[18] A pre-industrial control simulation of the GFDL CM2.1 global coupled GCM, run for 2000 yr with its atmospheric composition, solar irradiance, and land cover held fixed at 1860 values, shows strong interdecadal and intercentennial modulation of its ENSO behavior. This sampling variability attaches large uncertainties to certain ENSO metrics – such as the NINO3 SST variance and spectrum – diagnosed from centennial and shorter records. A null hypothesis for the slow modulation is that it arises from Poisson statistics applied to ENSO's seasonal phase-locking and interannual memory, the latter associated with ENSO's delayed recharge and modal time scales. This hypothesis must be weighed against alternatives – e.g., that separate decadal climate modes alter ENSO stability, that ENSO acts to regulate the tropical climatology, or that past ENSO modulation has resulted from orbital or anthropogenic forcings.

[19] Toward the IPCC Fifth Assessment, GFDL has developed several new CGCMs (CM2M, CM2G, and CM3), each of which uses either a different atmosphere or a different ocean than CM2.1. Preliminary control runs from these models also exhibit centennial-scale modulation of ENSO, as does a 700 yr run from the NCAR CCSM3.5 CGCM (B. Fox-Kemper, personal communication, 2008). If this is the case with other CGCMs – such as those in the CMIP3 archive – then model evaluation and intercomparison may require large ensembles or long runs (5 centuries or more) to expose robust changes in ENSO. More worryingly, if nature's ENSO is similarly modulated, there is no guarantee that the 150 yr historical SST record is a fully representative target for model development.

[20] The climate community could meet these challenges in several ways. Longer and more densely-sampled paleo records could illuminate the behavior of ENSO farther back

in time. More extreme tests of climate models – e.g., under mid-Holocene or glacial conditions – could produce larger ENSO changes that are more detectable in the face of sampling uncertainty. Alternate ENSO metrics – such as assimilation and forecast skill, or regressions scaled by ENSO amplitude – could highlight mechanisms with less sampling variability than that associated with ENSO spectra.

[21] That internally-generated modulation of ENSO may exist even with fixed climate forcings, does not preclude additional impacts of external perturbations – like orbital variations and anthropogenic forcings – which have been demonstrated to affect ENSO in climate models [*Guilyardi et al.*, 2009]; internally-generated modulation simply makes it more challenging to detect these effects. In any case, it is sobering to think that even absent any anthropogenic changes, the future of ENSO could look very different from what we have seen so far.

References

An, S.-I., J.-S. Kug, Y.-G. Ham, and I.-S. Kang (2008), Successive modulation of ENSO to the future greenhouse warming, *J. Clim.*, 21, 3–21.

Brown, J., M. Collins, A. W. Tudhope, and T. Toniazzo (2008), Modelling mid-Holocene tropical climate and ENSO variability: Towards constraining predictions of future change with palaeo-data, *Clim. Dyn.*, 30, 19–36.

Cane, M. A. (2005), The evolution of El Niño, past and future, *Earth Planet. Sci. Lett.*, 230, 227–240.

Cane, M. A., S. E. Zebiak, and Y. Xue (1995), Model studies of the long-term behavior of ENSO, in *Natural Climate Variability on Decade-to-Century Time Scales*, pp. 442–457, Natl. Acad. Press, Washington, D. C.

Delworth, T. L., et al. (2006), GFDL's CM2 global coupled climate models. Part I: Formulation and simulation characteristics, *J. Clim.*, 19, 643–674.

Fang, Y., J. C. H. Chiang, and P. Chang (2008), Variation of mean sea surface temperature and modulation of El Niño–Southern Oscillation variance during the past 150 years, *Geophys. Res. Lett.*, 35, L14709, doi:10.1029/2008GL033761.

Guilyardi, E. (2006), El Niño-mean state-seasonal cycle interactions in a multi-model ensemble, *Clim. Dyn.*, 26, 329–348.

Guilyardi, E., A. Wittenberg, A. Fedorov, M. Collins, C. Wang, A. Capotondi, G. J. van Oldenborgh, and T. Stockdale (2009), Under-

standing El Niño in ocean-atmosphere general circulation models: Progress and challenges, *Bull. Am. Meteorol. Soc.*, 90, 325–340.

Jin, F.-F. (1996), Tropical ocean-atmosphere interaction, the Pacific cold tongue, and the El Niño-Southern Oscillation, *Science*, 274, 76–78.

Jin, F.-F., J. D. Neelin, and M. Ghil (1994), El Niño on the devil's staircase: Annual subharmonic steps to chaos, *Science*, 264, 70–72.

Jin, F.-F., S.-I. An, A. Timmermann, and J. Zhao (2003), Strong El Niño events and nonlinear dynamical heating, *Geophys. Res. Lett.*, 30(3), 1120, doi:10.1029/2002GL016356.

Kleeman, R. (2008), Stochastic theories for the irregularity of ENSO, *Philos. Trans. R. Soc., Ser. A*, 366, 2511–2526.

Knutson, T. R., S. Manabe, and D. Gu (1997), Simulated ENSO in a global coupled ocean-atmosphere model: Multidecadal amplitude modulation and CO_2 sensitivity, *J. Clim.*, 10, 138–161.

Min, S.-K., S. Legutke, A. Hense, and W.-T. Kwon (2005), Internal variability in a 1000-yr control simulation with the coupled climate model ECHO-G. II. El Niño Southern Oscillation and North Atlantic Oscillation, *Tellus, Ser. A*, 57, 622–640.

Reichler, T., and J. Kim (2008), How well do coupled models simulate today's climate?, *Bull. Am. Meteorol. Soc.*, 89, 303–311.

Rodgers, K. B., P. Friederichs, and M. Latif (2004), Tropical Pacific decadal variability and its relation to decadal modulations of ENSO, *J. Clim.*, 17, 3761–3774.

Schopf, P. S., and R. J. Burgman (2006), A simple mechanism for ENSO residuals and asymmetry, *J. Clim.*, 19, 3167–3179.

Smith, T. M., R. W. Reynolds, T. C. Peterson, and J. Lawrimore (2008), Improvements to NOAA's historical merged land-ocean surface temperature analysis (1880–2006), *J. Clim.*, 21, 2283–2296.

Timmermann, A., J. Oberhuber, A. Bacher, M. Esch, M. Latif, and E. Roeckner (1999), Increased El Niño frequency in a climate model forced by future greenhouse warming, *Nature*, 398, 694–697.

Timmermann, A., F.-F. Jin, and J. Abshagen (2003), A nonlinear theory for El Niño bursting, *J. Atmos. Sci.*, 60, 152–165.

Tziperman, E., M. A. Cane, and S. E. Zebiak (1995), Irregularity and locking to the seasonal cycle in an ENSO prediction model as explained by the quasi-periodicity route to chaos, *J. Atmos. Sci.*, 52, 293–306.

van Oldenborgh, G. J., S. Y. Philip, and M. Collins (2005), El Niño in a changing climate: A multi-model study, *Ocean Sci.*, 1, 81–95.

Wittenberg, A. T. (2002), ENSO response to altered climates, Ph.D. thesis, 475 pp., Princeton Univ., Princeton, N. J.

Wittenberg, A. T., A. Rosati, N.-C. Lau, and J. J. Ploshay (2006), GFDL's CM2 global coupled climate models. Part III: Tropical Pacific climate and ENSO, *J. Clim.*, 19, 698–722.

Yukimoto, S., and Y. Kitamura (2003), An investigation of the irregularity of El Niño in a coupled GCM, *J. Meteorol. Soc. Jpn.*, 81, 599–622.

———————

A. T. Wittenberg, Geophysical Fluid Dynamics Laboratory, NOAA, P.O. Box 308, 201 Forrestal Road, Princeton, NJ 08542-0308, USA. (andrew.wittenberg@noaa.gov)